

XPS study of an intergranular phase in yttria-zirconia

A. E. HUGHES, B. A. SEXTON

CSIRO Division of Materials Science and Technology, Locked Bag 33, Clayton, Victoria, Australia, 3168

X-ray photoelectron spectroscopy (XPS) has been used to investigate impurity phase segregation at grain boundaries in 10 mol% Y_2O_3 -90 mol% ZrO_2 . The segregant material forms a thin film in the intergranular region up to 1400°C. At higher temperatures it redisperses to triple points and the external surface of the compacts used in the experiment. The XPS results indicate that the segregant material is similar to a chain silicate of composition $1.5Na_2O : 0.5Y_2O_3 : 3.0SiO_2$.

1. Introduction

Recently Badwal and Drennan [1] found anomalous behaviour in the ionic conducting properties of yttria-stabilized zirconia as a function of sintering temperature. They used impedance dispersion analysis to probe the conductivity across grain boundaries as well as the lattice conductivity. They observed that the grain-boundary resistivity showed an inflection as a function of sintering temperature near 1500°C which they attributed to a change in the location and morphology of a grain-boundary impurity phase. Below 1500°C the phase is uniformly dispersed as a thin film (1.2 nm) at the grain boundaries. Above 1500°C the grain-boundary phase is observed to dewet the boundary and redeposit itself at triple points and other lower energy sites. Energy dispersive X-ray analysis in the electron microscope was incapable of identifying the phase in the intergrain region below 1400°C but indicated that the material segregating at the triple points was silicon- and yttrium-rich.

In this study, X-ray photoelectron spectroscopy (XPS) has been used in an attempt to identify the composition of the intergranular phases. XPS is a surface specific technique, probing from 0 to 5 nm of the surface region in most solids [2]. It is ideally suited to the examination of surface-segregated phases, particularly if the phase is dispersed over a relatively large area. In recent years, X-ray induced Auger line kinetic energies have been combined with core level binding energy measurements to produce two-dimensional chemical state plots [3, 4]. These plots enable the identification of chemically similar surface phases by virtue of the shifts in the modified Auger parameter, α' [4]. Changes in α' reflect changes in the extra atomic relaxation energy which is dependent on the first coordination sphere of the ion in question. In the present study we have measured silicon α' values based on the Si *KLL* Auger line and the Si 2p photoelectron line to attempt the identification of silicon-containing impurity phases in yttria-zirconia.

2. Experimental procedure

The high-purity fine-grained prereacted powder with

a composition of 10 mol% Y_2O_3 + 90 mol% ZrO_2 (Viking Chemicals Ltd, Denmark) was pressed into either discs of 10 mm diameter and 2 mm thickness or modulus of rupture (MOR) bars of 50 mm length by 5 mm square cross-section. The compacts were then fired in an argon atmosphere in a conventional tube furnace at temperatures ranging from 1300 to 1700°C. The heating rate was 300°C h⁻¹ and samples were held at the target temperature for 15 h then cooled at 300°C h⁻¹, essentially reproducing the conditions described by Badwal and Drennan [1]. Although the Viking powder was quoted to be of high purity, the experimental evidence for a foreign intergranular phase resulted in extensive analysis for impurities by Badwal and Drennan. Of all the impurities detected, silicon (20 p.p.m.) and sodium (700 p.p.m.) are the only impurities pertinent to this study.

The reference sodium-yttrium-silicates were prepared by the method described by Cervantes *et al.* [5]. Analytical grade powders of quartz, Na_2CO_3 and Y_2O_3 were weighed out according to the required stoichiometry, ground under methanol in a mortar, dried, placed in platinum crucibles and then fired in air to 1500°C in an electrically heated muffle furnace. The crystalline forms of $Na_3YSi_3O_9$ and $Na_3YSi_2O_7$ were easily prepared by slow cooling from 1500°C. X-ray diffraction (XRD) on powdered samples confirmed that they were single-phase material. The glassy forms $1.5Na_2O : 0.5Y_2O_3 : 3.0SiO_2$, $1.5Na_2O : 0.5Y_2O_3 : 2.0SiO_2$ and $1.5Na_2O : 0.5Y_2O_3 : SiO_2$ were prepared by rapidly quenching the molten liquid state (1500°C) to ambient temperature by immersion in cold water.

Intergranular fracture surfaces were generated by two different methods. The methods included (i) three-point fracture and (ii) thermal downshock where the samples were rapidly quenched from 1000 to -196°C (liquid nitrogen). In all cases it was impossible to obtain 100% intergranular fracture. For samples fired at 1600 and 1700°C the amount of intergranular fracture to the total fracture surface was in excess of 80%. For samples fired in the 1300 to 1500°C range all the results presented were averaged over several fracture surfaces with 45 to 70% intergranular fracture.

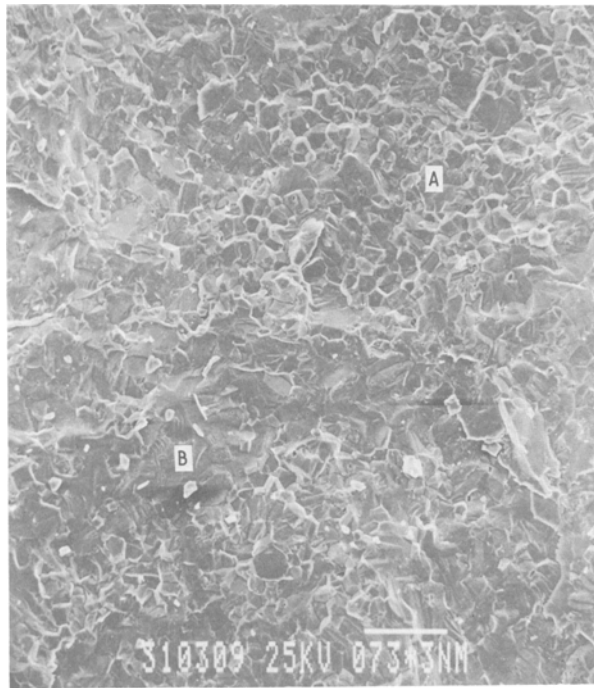


Figure 1 Scanning electron micrograph of a representative $Y_2O_3-ZrO_2$ fracture surface which has been heated to $1600^\circ C$ prior to fracture. Region A is predominantly intergranular fracture and region B transgranular fracture.

Error bars presented for the XPS results on the fracture surfaces take account of the variable amount of intergranular fracture. The amount of intergranular fracture on the fracture surface was determined by scanning electron microscopy (SEM). Fig. 1 displays the fracture surface of a sample fired at $1600^\circ C$ where region A is typical of intergranular fracture and region B typical of transgranular fracture.

X-ray photoelectron spectra were measured in a vacuum generators ESCALAB with an $AlK\alpha$ X-ray source ($1486.6 eV$, $150 W$) operating at a pressure of 7×10^{-10} torr. Samples were mounted with either double-sided tape or held in a metal spring loaded clamp, spot welded to the top of the sample stub. The Zr 3d line ($182.2 eV$) was used as a reference to correct for sample charging. The value of $182.2 eV$ was established with reference to the Au 4f7/2 line from gold evaporated on to a pellet pressed from the yttria-zirconia powder. Care was taken to eliminate relaxation effects [6] by evaporating successively higher doses of gold on to the sample until the Au 4f7/2 binding energy remained constant. This method gave binding energies of $157.7 eV$ for Y 3d5/2 and $284.6 eV$ for C 1s.

XPS atom number ratios were calculated using the formula

$$\frac{n(A)}{n(B)} = \frac{I(A) \sigma(B)}{I(B) \sigma(A)} \quad (1)$$

where $n(A)$ is the number of atoms of species A , $I(A)$ is the integral intensity of species A and $\sigma(A)$ is the photo-ionization cross-section [7]. Owing to the overlap of the Y 3d and Si 2p photoelectron peaks, the Y 3d intensity had to be extracted from the envelope of the two peaks by a curve-fitting technique described by Hughes and Sexton [8].

3. Results and discussion

The Y/Zr, Si/Zr and Na/Zr atom number ratios as a function of firing temperature for the external as-fired surface of the compacts (hereafter referred to as the "external" surface) as well as the fracture surface are displayed in Figs 2 and 3, respectively. On the external surface, the Y/Zr ratio is constant at 0.34 up to $1400^\circ C$ then rises to 0.37 above $1500^\circ C$. The Si/Zr and Na/Zr ratios both display maxima in their temperature dependence at 1500 and $1600^\circ C$, respectively, then decrease at higher temperatures. On the fracture surface (Fig. 3) the Y/Zr ratio increases from a value of 0.28 at $1300^\circ C$ to a maximum of 0.31 at $1400^\circ C$ then decreases up to $1600^\circ C$. Similarly the Si/Zr ratio increases from a value of 0.04 to $1300^\circ C$ to 0.17 at $1400^\circ C$ then decreases to zero at $1600^\circ C$ and above. The Na/Zr ratio increases from a value of 0.048 at $1300^\circ C$ to a peak value of 0.12 at $1400^\circ C$ then decreases to zero at $1600^\circ C$ and above.

The behaviour observed for the atom number ratios in Figs 2 and 3 may be explained in the following manner. Silicon, yttrium and sodium redisperse from the bulk of the material over the grain-boundary interface as the temperature increases. Peaking in the temperature dependence of yttrium, sodium and silicon on the fracture surface is probably due to a combination of loss of surface area due to grain growth but more importantly to a more homogeneous spreading of the material over the grain interface. It was in this region (1300 to $1600^\circ C$) that Badwal and Drennan [1] observed the impurity phase progressively change

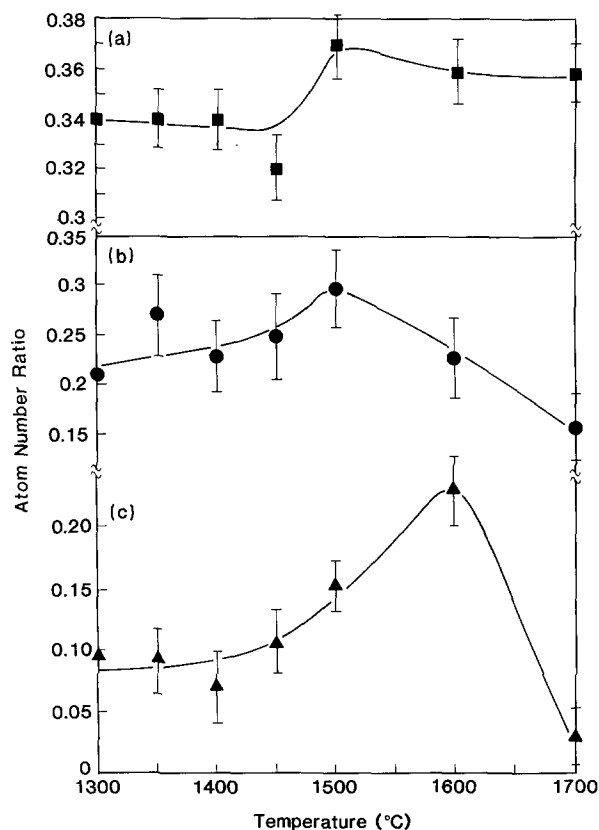


Figure 2 XPS atom number ratios for (a) Y/Zr, (b) Si/Zr and (c) Na/Zr on the external surfaces of 10 mol % $Y_2O_3-ZrO_2$ compacts as a function of the firing temperature. Results presented are the average of several experiments and the error bars represent the spread of results.

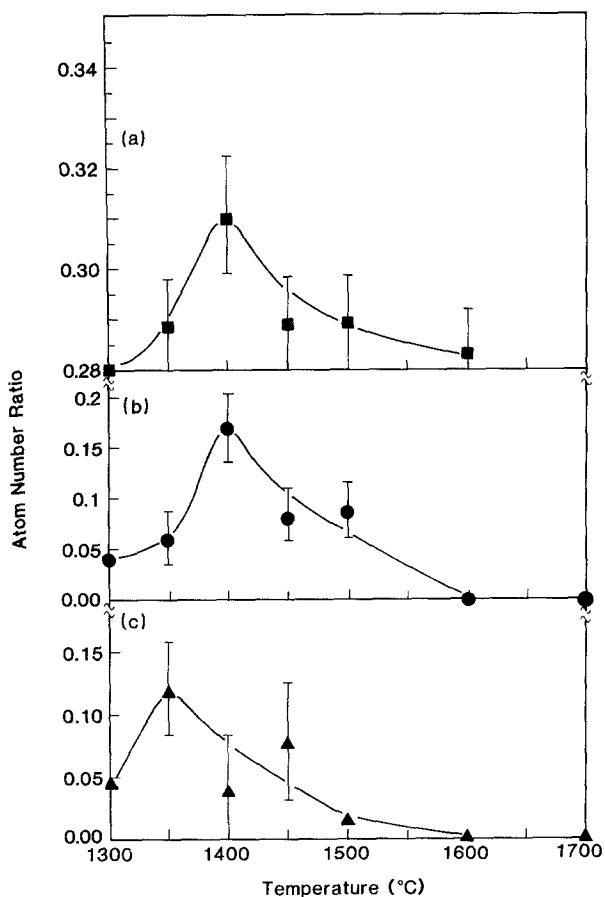


Figure 3 XPS atom number ratios for (a) Y/Zr, (b) Si/Zr and (c) Na/Zr on the fracture surfaces of 10 mol % $Y_2O_3-ZrO_2$ compacts as a function of the firing temperature.

from being a uniformly dispersed film at low firing temperatures to becoming large isolated pockets of material along grain boundaries and triple points at higher firing temperatures. EDAX analysis of the material at the triple points indicated that it was silicon- and yttrium-rich [1]. The similarity in behaviour of the silicon and yttrium dependence over the 1300 to 1500°C range indicate that the material observed by XPS is also yttrium- and silicon-rich with a strong possibility of compound formation between the two. Yttrium silicate or sodium yttrium silicate (as sodium is also present in the intergranular region) are likely candidates. At 1600°C the grain-boundary region has apparently purged itself of the segregating phase (or phases) as demonstrated by the decrease to zero of the Si/Zr and Na/Zr ratios and the decrease from 0.31 to 0.28 of the Y/Zr ratio.

The data for the external surface in Fig. 2 provides complementary evidence that the morphology of the impurity phase has changed in the 1300 to 1600°C range. Increases in the Y/Zr, Si/Zr and Na/Zr ratios over the 1300 to 1500°C range demonstrate that a large amount of material has migrated out of the intergranular region and redeposited itself on the external surface. Chaim *et al.* [9] have also observed the segregation of an yttrium-rich silicate in yttria-zirconia. Over this temperature range, Badwal and Drennan observed the redeposition of an impurity phase at the triple points, but XPS is probably unable to detect this material because the total analysis area occupied by this material is very small. At tempera-

tures higher than 1500°C the decrease in the Si/Zr and Na/Zr ratios is probably due to decomposition and volatilization resulting in a loss of material from the external surface. The fact that the Y/Zr signal remains constant above 1500°C suggests that during decomposition a non-volatile yttrium decomposition product has been left behind.

A semiquantitative estimate of the Si/Y ratio of the impurity phase may be obtained from the data in Figs 2 and 3. On the external surface the difference in the Si/Zr level at 1500°C compared to 1300°C represents the amount of silicon which has segregated to the external surface over that temperature range. The value is approximately 0.09. Similarly a value of 0.03 is obtained for the Y/Zr ratio, hence the Si/Y ratio is approximately 3. On the fracture surface, an analogous treatment for material that has redispersed on to the grain-boundary interface between 1300 and 1400°C yields a value of 4 for the Si/Y ratio. As an average for both surfaces the impurity phase has an approximate ratio of Si/Y of 3.5.

The spectroscopic results for the external and fracture surfaces are plotted along with a number of reference compounds and regions on a two-dimensional chemical state plot for silicon in Fig. 4 [4]. The two-dimensional chemical state plot graphs the Si 2p binding energy against the Si(KLL) Auger kinetic energy (generated by Bremsstrahlung radiation [4]). Both peaks contain oxidation state information as well as information on the ability of surrounding electron density to screen the final state configuration generated by the photoelectric and Auger processes. As a consequence they can indirectly give structural information for different classes of compounds. Hence the silicas, quartz, (Q) and aerosil (A), which fall in the bottom left-hand corner of the plot, are well separated from sheet silicates (region I) and chain silicates (region II) [4]. Included on the plot are a number of reference sodium yttrium silicates: (1) $Na_3YSi_2O_7$ which is a dimeric ion silicate; (2) $Na_3YSi_3O_9$, an infinite chain silicate; and (3) $Na_3YSi_2O_5$ which is compositionally a sheet silicate. The letters X and G denote the crystalline and glassy states of these materials as determined by X-ray diffraction [5]. The diagonal lines on the two-dimensional chemical state plot are lines of constant Auger parameter and essentially represent similar ability of neighbouring atoms to screen final state ions.

The results taken on the grain boundary (\square) and external surfaces (\circ) are also presented in Fig. 4. As no trend can be distinguished between the results obtained on both types of surface, it can be deduced that the impurity phase forming at the grain boundary is the same as that segregating to and forming on the external surface. The nature of this material can immediately be identified by its position on the two-dimensional chemical state plot. As a group the data for both the fracture and the external surfaces lies in a region attributed to the infinite chain silicates. The exact silicate cannot be positively identified from its plot position. However, the previous Si/Y stoichiometry of 3.5 makes $1.5Na_2O:0.5Y_2O_3:3.0SiO_2$ the most likely phase. Infinite sheet and framework silicates

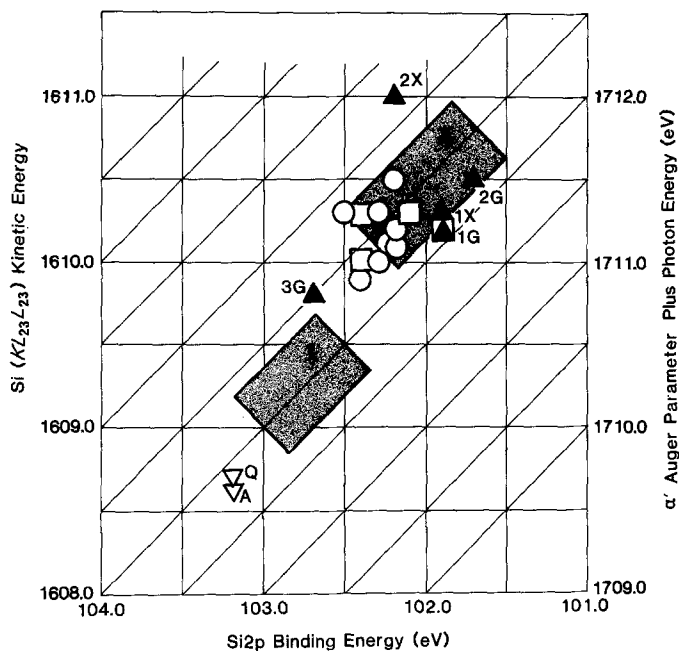


Figure 4 Two-dimensional chemical state plot for silicon compounds. Reference regions and compounds are defined as follows: Q = quartz; A = aerosil; Region I, infinite sheet silicates; Region II, infinite chain silicates. (▲) Reference silicates. 1, $\text{Na}_3\text{YSi}_3\text{O}_9$; 2, $\text{Na}_3\text{YSi}_2\text{O}_7$; 3, $\text{Na}_3\text{YSi}_2\text{O}_5$, G = glassy phase. X = Crystalline phase; (○) external surface of $\text{Y}_2\text{O}_3\text{-ZrO}_2$ compacts; (◻) fracture surface of $\text{Y}_2\text{O}_3\text{-ZrO}_2$ compacts.

can definitely be ruled out. The formation of zirconium–yttrium–sodium silicates seems unlikely for two reasons. First, a much higher Si/Y ratio would be expected in a chain silicate if some of the yttrium atoms were replaced by zirconium atoms. Second, the EDAX measurements on the material at the triple points indicated only yttrium and silicon enrichment but no zirconium enrichment [1].

The role of sodium, however, is still unclear because the Na/Zr ratios on both surfaces do not follow the trends displayed by the silicon and yttrium. This is not surprising, because in the formation of the silicate $1.5\text{Na}_2\text{O} : 0.5\text{Y}_2\text{O}_3 : 3.0\text{SiO}_2$, sodium and silicon react in a 1:1 ratio but sodium occurs at 35 times the impurity level of silicon in the Viking material. Thus most of the excess sodium must occur in other forms possibly Na_2O or Na_2ZrO_3 [10]. The spectroscopic data for sodium provides a much less sensitive probe to the atomic environment than silicon. Thus no direct useful information can be gleaned from the sodium spectroscopic data on compound formation at the intergranular region. Na_2O is known to be a flux for the reaction of Y_2O_3 and SiO_2 [11] which raises the possibility that if Na_2O is present at the intergrain region then yttrium silicate may form rather than sodium yttrium silicate. Three factors mitigate against the formation of an yttrium silicate and possibly the presence of Na_2O . First, the Si/Y ratio measured by XPS is much higher than would be expected for an yttrium silicate. Second, the spectroscopic results indicate the formation of a chain silicate and not $\text{Y}_2(\text{SiO}_4)\text{O}$, the reaction product found by Leskela and Jyrkas [11] where they employed Na_2O as a flux in the formation of yttrium silicates. Third, Na_2O volatilizes from the reactants under the conditions of the experiment described by Leskela and Jyrkas, an option which does not exist at the intergranular interface. A further reason for rejecting the presence of Na_2O is provided by the data in Fig. 2 for the Na/Zr ratio on the external surface of the compacts. Fig. 2 clearly displays that sodium is present up to 1600°C , which is well above the melting point of Na_2O [12],

making it unlikely that sodium is present as Na_2O . The viability of Na_2ZrO_3 as a phase at 1600°C is also unclear from the literature. Suzuki *et al.* [13] claim that Na_2ZrO_3 melts incongruently at $\sim 1180^\circ\text{C}$ whereas Sircar and Brett [10] and D'Ans and Loffler [14] claim that it is stable up to $\sim 1500^\circ\text{C}$ which would provide better agreement with the results presented in Fig. 2. In summary, the evidence suggests that two likely intergranular impurity phases present in the yttria–zirconia after firing at elevated temperatures are an infinite chain silicate most closely related to the composition $1.5\text{Na}_2\text{O} : 0.5\text{Y}_2\text{O}_3 : 3.0\text{SiO}_2$ and sodium zirconate.

An unusual feature of the Y/Zr ratios is the high initial values at 1300°C of 0.28 and 0.34 for the fracture and external surfaces, respectively. Even the unfired uncompact powder had an Y/Zr ratio of 0.36 which is well above the bulk value of 0.22 obtained from chemical analysis of the Viking powder. XPS depth profiling experiments displayed an Y/Zr ratio decreasing to the bulk value as a function of depth. The focal point of the discussion of the yttrium segregation is its consequence on properties such as the grain-boundary resistivity, due to increased solubility of impurity atoms in an yttrium-rich material or crystallographic changes (tetragonal to cubic) for low mol % solid solutions [9]. The origin of the yttrium segregation is the subject of further investigation by us.

4. Conclusions

X-ray photoelectron spectroscopy has been used to identify an intergranular silicate material in yttria–zirconia. The existence of an intergranular material had previously been invoked to explain anomalous behaviour in the grain-boundary resistivity as a function of firing temperature and hence grain size [1]. XPS, through the measurement of the silicon, yttrium and sodium signals has been able to track the emergence and dispersion of the silicate as a thin film in the intergranular region up to 1400°C . Above 1400°C the material undergoes a redispersion to triple points and

to the exterior of compacts of the yttria-zirconia. The identification by XPS of the silicate material as being similar to $1.5\text{Na}_2\text{O} : 0.5\text{Y}_2\text{O}_3 : 3.0\text{SiO}_2$ agrees well with the observed cleaning temperature of the grain boundaries, because for the $\text{Na}_2\text{O}-\text{Y}_2\text{O}_3-\text{SiO}_2$ system the liquidus temperature is 1450°C [5]. Above 1500°C the grain boundaries are essentially clean of silicate material although larger pockets of material have been identified at triple points [1]. On the external surface much of the impurity silicate as well as sodium zirconate volatilizes above 1600°C leaving the external surface much cleaner of impurity compounds.

This study demonstrates that XPS is an extremely useful adjunct to other techniques for the study of ceramic materials, particularly when the properties of the ceramic under scrutiny, such as grain-boundary resistivity, are likely to be associated with morphologies of the material amenable to surface analysis techniques.

Acknowledgements

We thank Dr S. Badwal and Dr J. Drennan for useful discussion concerning the results and critical reading of the text. We also thank Dr Badwal for supplying us with the yttria-zirconia powder as well as time on the molybdenum tube furnace.

References

1. S. BADWAL and J. DRENNAN, *J. Mater. Sci.* **22** (1987) 3231.
2. E. D. HONDROS and M. P. SEAH, *Int. Met. Rev.* **222** (1977) 262.
3. C. D. WAGNER, L. H. GALE and R. H. RAYMOND, *Anal. Chem.* **51** (1979) 466.
4. C. D. WAGNER, D. E. PASSOJA, H. F. HILLERY, T. G. KINISKY, H. A. SIX, W. T. JENSEN and J. A. TAYLOR, *J. Vac. Sci. Technol.* **21** (1982) 933.
5. F. CERVANTES, L. J. MARR and F. P. GLASSER, *Ceram. Int.* **7** (2) (1981) 43.
6. S. KOHIKI and K. OKI, *J. Electron Spectrosc. Relat. Phenom.* **36** (1985) 105.
7. J. H. SCOFIELD, *ibid.* **8** (1976) 129.
8. A. E. HUGHES and B. A. SEXTON, *ibid.* (1987) **46** (1988) 31.
9. R. CHAIM, D. G. BRANDON and A. H. HEUER, *Acta Metall.* **34** (1986) 1933.
10. A. SIRCAR and N. H. BRETT, *Trans. Brit. Ceram. Soc.* **69** (3) (1970) 133.
11. M. LESKELA and K. JYRKAS, *J. Amer. Ceram. Soc.* **70** (1987) C160.
12. R. C. WEAST and M. J. ASTLE (eds) "C.R.C. Handbook of Chemistry and Physics", 61st Edn (CRC, Boca Raton, Florida, 1980-81).
13. H. SUZUKI, S. KIMURA, H. YAMADA and T. YAMAUCHI, *J. Jpn Ceram. Soc.* **69** (1961) 52.
14. J. D'ANS and J. LOFFLER, *Z. Anorg. Allgem. Chem.* **191** (19) (1930) 135.

Received 4 January
and accepted 6 May 1988